Mat. Res. Soc. Symp. Proc. Vol 627 © 2000 Materials Research Society

A Simple Description of Thick Avalanches at the Surface of a Granular Material

Achod Aradian, Elie Raphaël and Pierre-Gilles de Gennes

Laboratoire de Physique de la Matière Condensée, URA n°792 du C.N.R.S., Collège de France, 11 place Marcelin Berthelot, 75231 Paris Cedex 05, France

e-mail: Achod.Aradian@college-de-france.fr, Elie.Raphael@college-de-france.fr, Pierre-Gilles.deGennes@espci.fr

ABSTRACT

Some years ago, Bouchaud *et al.* introduced a phenomenological model to describe surface flows of granular materials [J. Phys. Fr. I **4**, 1383 (1994)]. According to this model, one can distinguish between a static phase and a rolling phase that are able to exchange grains through an erosion/accretion mechanism. Later, Boutreux *et al*. [Phys. Rev. E **58**, 4692 (1998)] proposed a modification of the exchange term in order to describe thicker flows where saturation effects are present. However, these two approaches assumed that the downhill convection velocity of the grains is constant inside the rolling phase, a hypothesis that is not verified experimentally. We have recently modified the above models by introducing a velocity profile in the flow, and analyzed the physical consequences of this modification in the simple situation of an avalanche in an open cell. We here emphasize the physical predictions of our model, and show, in particular, that the thickness of the avalanche depends strongly on the velocity profile.

A SIMPLE MODEL FOR THICK AVALANCHES

Onset of avalanches

It is well-known that the top surface of a sand heap need not be horizontal, unlike that of a stagnant liquid. However, there exists an upper limit to the slope of the top surface, and the angle between this maximum slope and the horizontal is known, for non-cohesive material, as the Coulomb critical angle θ_{max}. Above this angle, the material becomes unstable, and an avalanche

at the surface might occur. The Coulomb angle is related to the friction properties of the material through $\tan\theta_{max} = \mu_i$, where μ_i is an internal friction coefficient [1].

As of today, the physical picture associated with the onset of the avalanche is still obscure. One could imagine a local scenario in which the dislodgement of some unstable grains leads by amplification to a global avalanche (see for instance [2]). Alternately, one can think of a delocalized mechanism [3], in which a thin slice of material is destabilized and starts to slide as a whole. In the present paper, we will focus on the latter point of view.

It has been recently suggested [3] that the thickness of the initial gliding layer should be of the order of ξ, the mesh size of the contact force network [4]. For simple grain shapes (spheroidal), one expects ξ ~5-10 grain diameter d. The angle at which the avalanche process actually starts would then be of the order of $\theta_m + \xi / L$, where L is the size of the free surface. At the moment of onset, our picture is that this initial layer starts to slip, and is rapidly fluidized by the collisions with the underlying heap, therefore generating a layer of rolling grains on the whole surface.

Now that we have proposed a description of the initial situation, we may turn to the model scheme accounting for the further evolution of the avalanche.

Saturation effects for thick avalanches

Some years ago, Bouchaud, Cates, Ravi Prakash and Edwards introduced a model to describe surface flows of granular materials [5]. The model assumes a rather sharp distinction between *immobile* particles and *rolling* particles and, accordingly, introduces the following two important physical quantities (see Figure 1): the local height of immobile particles h(x,t) (where x denotes the horizontal coordinate[1] and t the time), and the local amount of rolling particles R(x,t). The time evolution of h(x,t) is written in the form

$$\frac{\partial h}{\partial t} = \gamma R(\theta_n - \theta) \qquad (1)$$

where $\theta \approx \tan\theta = \partial h / \partial x$ is the local slope, γ a characteristic frequency and θ_n the neutral angle of grains at which erosion of the immobile grains balances accretion of the rolling grains. For the

[1] In this article, we restrict ourselves to two-dimensional sandpiles.

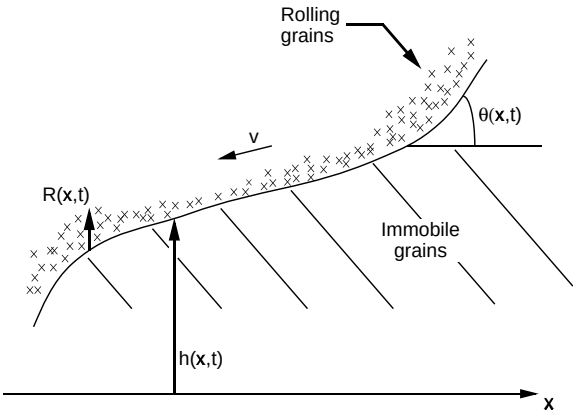

Figure 1. *The basic assumption of the BCRE picture is that there is a sharp distinction between immobile grains with a profile* $h(x,t)$*, and rolling particles with a local amount* $R(x,t)$*. The immobile grains consitute the "static phase" and the rolling ones the "rolling phase". The local slope of the static profile is called* $\theta(x,t)$*.*

rolling particles, Bouchaud and co-workers wrote a convection-diffusion equation [5] that was later simplified by de Gennes as [6]

$$\frac{\partial R}{\partial t} = v\frac{\partial R}{\partial x} - \frac{\partial h}{\partial t} \qquad (2)$$

where v is the downhill typical velocity of the flow, assumed to be constant.

According to the Bouchaud-Cates-Ravi Prakash-Edwards (BCRE) model, $\partial h / \partial t$ is linear in R (see Eq. 1). This is natural at small R, when all the rolling grains interact with the immobile particles. But as explained in Refs. [7,8], this cannot hold when R becomes larger than a given *saturation length* ξ', since the grains in the upper part of the rolling phase are no longer in contact with the immobile grains. The length ξ' is expected[2] to be of the order of a few grain diameters d. This led Boutreux, Raphaël, and de Gennes to propose [8] a modified *saturated* version of the BCRE Eq. 1, valid for thick surface flows and of the form

$$\frac{\partial h}{\partial t} = v_{uh}(\theta_n - \theta) \qquad (R >> \xi'), \qquad (3)$$

where v_{uh} is defined by $v_{uh} \equiv \gamma \xi'$. The constant v_{uh} has the dimensions of a velocity (where the subscript "uh" stands for uphill).

The description of thick avalanches modelized by Eq. 3 was discussed in Ref. [8]. However, one might encounter situations where the local amount R of rolling particles is rather large except in some regions of space where it takes values smaller than ξ'. For such cases, various

[2] One expects ξ' to be somewhat smaller than ξ, see [17].

"generalized" forms of the BCRE equations valid both in the large and small R limit, and able to handle intermediate values have been proposed [7,9,10]. As we will be mainly concerned with thick flows, we will here use the saturated form (Eq. 3).

Velocity profiles in thick flows

We now consider the hypothesis made in Eq. 2 that the downhill typical convection velocity of the rolling grains v is constant. As a matter of fact, v might vary for two reasons.

First, v depends on the local slope $\partial h / \partial x$ of the static bed, reflecting that the mean convection velocity should increase as the sandpile is further tilted. However, in the situation we are going to consider, the slope should never depart from θ_n by more than a few degrees, so that the variations of v originating in this may reasonably be taken to be negligible.

Second, v might as well depend on the local amount of rolling particles R. This dependence is quite natural, since as soon as the thickness of the flow exceeds a few grain diameters, one would expect a velocity gradient perpendicular to the flow to establish. Such a possibility was already considered by Bouchaud *et al.* [10], but, to our best knowledge, not further studied. We think that taking this velocity gradient into account does lead to an improvement of the model description of avalanches. In the forthcoming sections we will analyse the physical consequences of this modification.

If analyticity is assumed, we can expand v(R) in powers of R, and considering only the first two contributions to be significant, we write:

$$v(R) = v_0 + \Gamma R \qquad (4)$$

with Γ a constant, homogeneous to a shear rate, and v_0 a constant velocity. When R becomes small, Eq. 4 tells us that v(R) becomes constant [$v(R) \to v_0$]. Physically, this velocity should correspond to the typical rolling velocity of a single grain on a bed of immobile grains. For simple grain shapes (spheroidal) and average levels of inelastic collisions, one expects this velocity v_0 to scale as $\sqrt{gd}$ (where g is the gravity) [6,11,12]. Similarly, the shear rate Γ is expected to scale as $\sqrt{gd}/d \approx \sqrt{g/d}$. We can therefore rewrite Eq. 4 as:

$$v(R) = \Gamma(R + d) \qquad (5)$$

We note that v_0 becomes negligible compared to ΓR as soon as R exceeds a few grain diameters.

In our approach, the typical velocity v(R) depends *linearly* on the local rolling height R. Such a form is in part motivated by the recent work of Douady *et al.* [13] (see also our concluding remarks). It is also supported by the experimental results of Rajchenbach *et al.* who carried measurements in a rotating drum [14,2]. These authors have found linear velocity profiles in the surface flow, with a shear rate Γ independent of the thickness of the flow. However, in other experiments of chute flows carried out on rough inclined planes, Azanza *et al.* [15] and Pouliquen [16] have observed that the mean velocity (averaged on cross-sections) scales as a power-law of the thickness with an exponent about 3/2. In the following we will mainly focus on the linear form of Eq. 5, since it allows us to give explicit analytical solutions, and shall discuss the changes that occur in the case of a power-law velocity later on.

In the next section, we will derive the governing equations from the saturated BCRE equations and the above considerations on the velocity profile inside the flow.

Governing equations

We may define a reduced profile $\tilde{h}$, deduced from h by substracting the "neutral" profile $\theta_n x$: $\tilde{h}(x,t) = h(x,t) - \theta_n x$. Using Eqs. 2, 3, and 5, we easily obtain the following system:

$$\frac{\partial \tilde{h}}{\partial t} = -v_{uh} \frac{\partial \tilde{h}}{\partial x}, \tag{6}$$

$$\frac{\partial R}{\partial t} = \Gamma(R+d) \frac{\partial R}{\partial x} + v_{uh} \frac{\partial \tilde{h}}{\partial x} \quad . \tag{7}$$

In our approach, these equations are the governing equations for surface avalanches displaying linear velocity profiles.

An important point is that we must have R > 0 for Eqs. 6 and 7 to be valid. If we reach R=0 in a certain spatial domain, then Eq. 6 must be replaced in that domain by $\partial \tilde{h} / \partial t = 0$.

CASE OF AN OPEN SYSTEM

Physical situation

Let us consider a cell, of dimension L, partially filled with monodisperse grains of diameter d, as shown on Figure 2. The heap has an initial uniform slope θ_{max}, the Coulomb angle of the

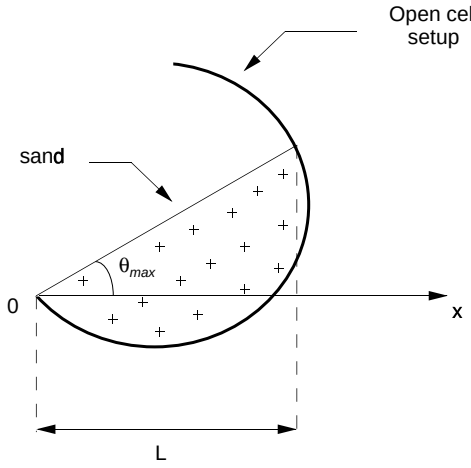

Figure 2 *Example of an open cell, so as to let the rolling material flow out at the bottom. We suppose that the avalanche starts precisely at* $\theta = \theta_{max}$.

material. The origin of the x-axis is taken at the bottom of the cell, and the orientation of the axis is such that the slope of the heap is positive.

Suppose that an avalanche has just started in the cell (as described above), so that we have at time t=0 a layer of rolling grains in the whole cell, of thickness $\sim \xi$ greater than the saturation length ξ'. We may thus use the saturated equations 6 and 7 from the beginning of the avalanche. As the rolling population will rapidly grow and become independent of the initial thickness ξ (for ξ small), we can as well consider the initial condition on R to be $R(x, t = 0) = 0$. We also know the initial value of $\tilde{h}$:

$$\tilde{h}(x, t = 0) = (\theta_{max} - \theta_n)x \equiv \eta x \qquad (8)$$

where η is defined as the (positive) difference between the Coulomb angle and the neutral angle. We have additional conditions in our system, due to the boundaries. At the top of the cell, there is no input of rolling species, so that we impose $R(x = L, t) = 0$ at any time $t \geq 0$. Another condition arises from the fact that grains fall off the cell at the bottom and cannot accumulate there, giving $\tilde{h}(x = 0, t) = 0$ at any time $t \geq 0$.

Uphill wave in the static phase

Equation. 6 can be readily solved along with the initial and boundary conditions on $\tilde{h}$ to give:

$$\tilde{h}(x, t) = \eta(x - v_{uh} t)\, H(x - v_{uh} t) \qquad \text{for } 0 \leq x \leq L, \qquad (9)$$

where H denotes the Heavyside unit step function [H(u)=1 if u>0, H(u)=0 otherwise] [3]. This result corresponds to the uphill propagation (at constant speed v_{uh}) of a surface wave on the static phase. Let us call $x_{uh}(t)$ the time-dependent position of the wavefront, given by $x_{uh}(t) = v_{uh} t$.

The wave starts from the bottom of the cell at time t=0 and reaches the upper end at a time t_2 defined by

$$t_2 \equiv L / v_{uh}. \qquad (10)$$

The profile of the static phase at a given time t, smaller than t_2, is pictured on Figure 3, and can be described as follows: ahead of the wavefront [$x_{uh}(t) \le x \le L$], the profile is linear with a slope given by the initial angle θ_{max} (since $\tilde{h} = \eta v_{uh}$). Behind the wavefront [$0 \le x \le x_{uh}(t)$], the slope has decreased and reached the neutral angle θ_n ($\tilde{h} = 0$). For times $t \ge t_2$, the slope of the static phase inside the cell is uniformly equal to the final value θ_n, which is thus the angle of repose of our specific open cell system.[4]

Downhill convection of rolling grains

Substituting Eq. 9 into the evolution equation for R (Eq. 7) gives:

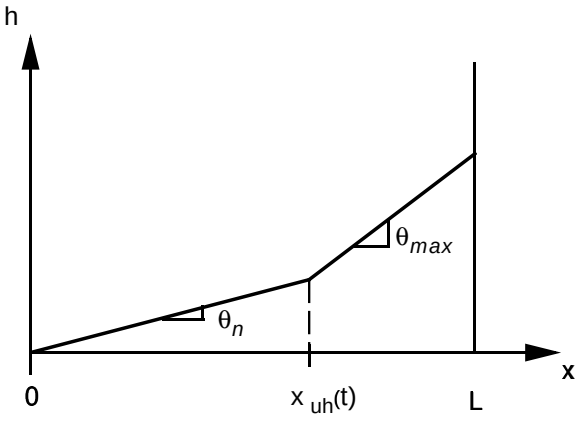

Figure 3. *The profile of the static phase for* $0 < t < t_2$. *At the left of* $x_{uh}(t)$, *the slope has relaxed to its final value* θ_n. *On the right of it, it still retains the initial angle* θ_{max}.

[3] Please note that Eq. 9 corrects Eq. 13 of Ref. [17], which contains a misprint.

[4] Boutreux *et al*. have shown in Ref. [8] that the notion of "repose angle" is not an intrinsic property of the material, but depends explicitly on the cell geometry.

$$\frac{\partial R}{\partial t} - \Gamma(R+d)\frac{\partial R}{\partial x} = \eta v_{uh} H(x - v_{uh} t). \qquad (11)$$

Equation 11 is a non-linear convection equation. The rolling species are thus convected downhill, with a convection velocity that depends on the local rolling thickness R. In the spatial region $x > v_{uh} t$, the right-hand side (which links the evolution of R to that of $\tilde{h}$) plays the role of a source term, leading to an amplification of the avalanche. On the contrary, for $x \le v_{uh} t$, the r.h.s. of Eq. 11 goes to zero, so that the material flowing through the surface $x = v_{uh} t$ from uphill is convected without amplification or damping.

Temporal evolution of the avalanche

To obtain a full analytical description of the avalanche evolution, one must solve Eq. 11 along with the two boundary conditions $R(x = L, t) = 0$ and $\tilde{h}(x = 0, t) = 0$. This has been done in Ref. [17], using the method of characteristics. In the present paper, however, we will focus on the essentiel physical features predicted by the model.

The influence of the bottom boundary condition $\tilde{h}(x = 0, t) = 0$ progressively invades the whole cell with a velocity v_{uh} (see Eq. 9 above). In a similar way, the influence of the top boundary condition $R(x = L, t) = 0$ propagates progressively from the top to the bottom of the cell (one can show that this propagation is uniformly accelerated, a direct consequence of the non-linearity in Eq. 11). The propagation of these boundary condition controls the different stages of the avalanche evolution. Figure 4, for example, illustrates what happens in the first stage of the avalanche. In the top region corresponding to $x_{dh}(t) \le x$, the flow is under the influence of the boundary condition at $x = L$. On the contrary, the bottom region [$x \le x_{uh}(t)$] is controlled by the boundary condition at $x = 0$, and the evolution equation region for R displays no more amplification (since the local slope has relaxed to its repose value). In the central region [$x_{uh}(t) \le x \le x_{dh}(t)$], the boundary conditions have no influence, and the rolling phase grows linearly with time.The overall shape of the rolling phase at the different stages of the avalanche is of course very dependent on the boundary condition for R at the top of the cell, but also on the condition for $\tilde{h}$ at the bottom, since the evolution of $\tilde{h}$ and R are coupled.

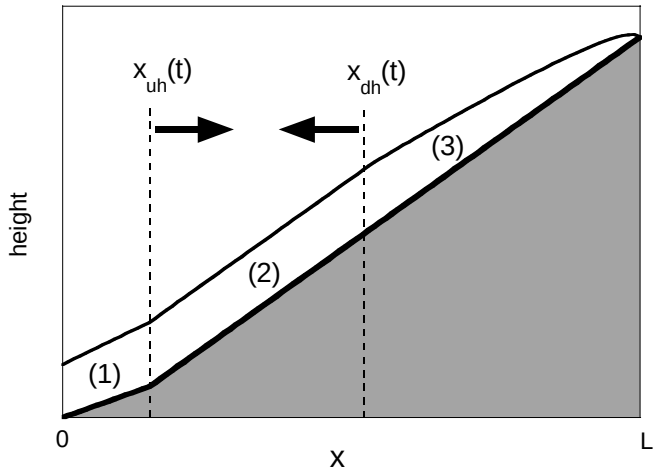

Figure 4. . *"Snapshot" of the avalanche during its first stage, from the full analytical solution: rolling phase (light) and static phase (dark).* $x_{uh}(t)$ *and* $x_{dh}(t)$ *represent the extension of boundary effects in the cell (respectively originating from the bottom and the top of the cell). The arrows symbolize the respective motion of the fronts. For clarity purposes, the thickness of the rolling part was augmented relatively to the static one.*

DISCUSSION AND SIMPLE CHECKS

From the full analytical solution of Eqs. 6 and 7 (presented in [17]), we can extract the following interesting physical quantities characterizing the avalanche evolution.

Avalanche duration

From the onset of the avalanche at $t = 0$ till time $t = t_2 = L / v_{uh}$, there exists a spatial region where the local slope of the pile has not yet relaxed to its repose value, thus leading to a net creation of rolling grains. In contrast, for times greater than t_2, the slope of the static part is θ_n everywhere in the cell, and no amplification of the moving grains can take place; the rolling phase existing at time t_2 is then simply convected downwards. Hence, the last grains to fall off the cell are those that had left the top end of the cell at time t_2. This event, which brings the avalanche to an end, occurs at time

$$t_{end} = t_2 + \frac{L}{\Gamma d}. \qquad (12)$$

Equation 12 gives the overall avalanche duration.

Predictions for the maximum thickness of the avalanche

Another interesting quantity is the maximum thickness R_{max} reached by the avalanche in the course of its evolution. If we consider flows displaying a linear velocity profile, the analytical expression for R_{max} is [17]

$$R_{max} = -d - \frac{v_{uh}}{\Gamma} + \sqrt{\left(d + \frac{v_{uh}}{\Gamma}\right)^2 + 2\eta \frac{v_{uh}}{\Gamma} L}. \qquad (13)$$

For large values of L, R_{max} scales as:

$$R_{max} \approx \sqrt{2\eta \frac{v_{uh}}{\Gamma} L}\,, \qquad (14)$$

that is, as the square root of the system size L.

Let us give some numerical applications of this last expression. For the case of a standard laboratory experiment, with L=1 m, d=1 mm, $v_{uh}/\Gamma = 3d$ and $\eta = 0.1$ rad, we find R_{max}=2.45 cm. In the case of a system at the scale of a desert dune, made of fine sand, we take L= 10 m, d=0.2 mm and, with others parameters unchanged, we get R_{max}=3.46 cm. One has to notice that R_{max} is quite small, even for large systems as a sand dune.

It is interesting to contrast this result with the work of Boutreux *et al*. [8], who carried out the same calculation in an open cell configuration, but with a constant downhill convection velocity $v(R) \sim v_0$ (instead of Eq. 4). They found $R_{max} \approx \eta L$. For the two above examples, this formula leads to maximum amplitudes of respectively 10 cm and 1 m. The effect of the velocity gradient is thus to considerably limit the amplitude of avalanches, especially for large systems.

In the beginning of this article, we quoted the work of Azanza *et al*. [15] and of Pouliquen [16] who find that the average speed for a granular material flowing on a rough plane is related to its thickness through a power-law relation $v(R) \approx \Gamma R^{\alpha}$ with an exponent α close to 3/2.[5] If

[5] As pointed out by Pouliquen [16], the influence of the rough underlying plane on the behaviour of the flow is rather complex and not yet fully understood. Our model, which assumes

we use such a power-law relation in our model, we find that R_{max} is expected to be of the order of

$$R_{max} \approx \left((\alpha+1)\eta \frac{v_{uh}}{\Gamma} L \right)^{\frac{1}{\alpha+1}}. \qquad (15)$$

Note that R_{max} diminishes as α increases. In particular, for α = 3/2, Eq. 15 can be rewritten as $R_{max} \approx (5\eta L v_{uh} / 2\Gamma)^{2/5}$.

Loss of material at the bottom of the cell

The loss of material at the bottom edge of the cell might be measured experimentally and compared with the following theoretical prediction. This loss corresponds to the flow rate at the bottom of the cell, and is given by:

$$Q(x=0,t) = \int_0^{R(x=0,t)} v(z)\, dz = \frac{\Gamma}{2} R(x=0,t)^2 + \Gamma d\, R(x=0,t)\ , \qquad (16)$$

where R(x=0,t) is obtained from the full analytical solution of Eqs. 6 and 7. Figure 5 shows the predicted shape of $Q(x=0,t)$ as a function of time (solid curve). For comparison, we also plotted, on the same figure, the curve obtained with the assumption of a constant downhill

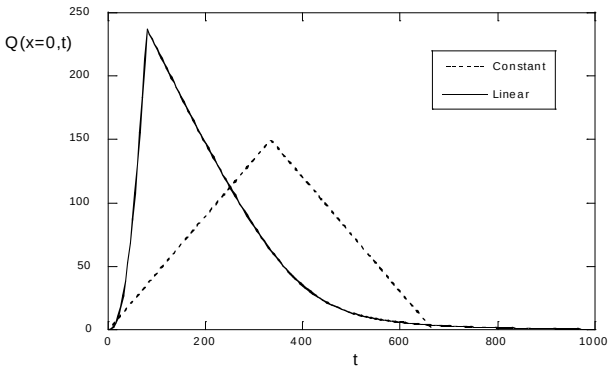

Figure 5. *Loss of material Q(x=0,t) at the bottom edge of the cell as a function of time. Solid line: predicted shape with a linear velocity profile in the flow. Dashed line: predicted shape in the case of a constant velocity (from Ref. [8]). Q is in units of* Γd^2*, t in units of* $1/\Gamma$.

---

that the flow takes place at the surface of a heap, might therefore not be appropriate to describe the experiments of Refs. [15] and [16].

velocity (dashed line) [8]. We observe that the solid curve displays a maximum corresponding to the moment when the maximum amplitude R_{max} rolls out of the cell. This maximum flow rate is obtained by replacing R(x=0,t) by R_{max} in Eq.16.

CONCLUDING REMARKS

Effects of polydispersity

It is of common knowledge that real granular materials are generally intrinsically polydisperse. This may have drastic effects on the behavior of the flow, and capturing more precisely the physics of real avalanches would certainly suppose to take polydispersity into account. However, the treatment of full polydispersity is a difficult task. Yet, the BCRE equations have been extended to the case of binary mixtures [18,19], and it could be interesting to study the changes brought up in this case by a velocity gradient in the flow.

Domain of validity of the BCRE approach

The general approach introduced by Bouchaud *et al*. to describe surface flows is rather phenomenological. In a recent work, Douady *et al*. [13] have extended the classical approach of Savage and Hutter [20] to physical situations, like the one considered in the present paper, where the boundary between the static part of the pile and the flowing one is unknown. For the particular case of a flow velocity linear in R, the model of Douady *et al*. allows one to recover the governing equations 6 and 7. For other cases, a supplementary term coupling the quantities R and h should be added to Eq. 6.

Other directions of study

Very recently, Dorogovtsev and Mendes [21] have analysed the progressive build-up of a sanpile using the thick flow equations 2 and 3. They have shown that space periodicity takes place while the sandpile evolves (the grains are piling layer by layer), even for a pile made of only one type of particles.

All our study was based on a thick flow assumption. The features generated by the nonlinear thin flow equation 1, such as conservation equations, or shock fronts propagation, have also been recently studied by Mahadevan and Pomeau [22], and by Emig, Claudin and Bouchaud [23].

ACKNOWLEDGEMENTS

We thank T. Boutreux, F. Chevoir, A. Daerr, S. Douady, J. Duran and O. Pouliquen for oral and/or written exchanges.

REFERENCES

[1] For a detailed description of the Coulomb approach and its extensions, see R.M. Nedderman, *Statics and Kinematics of Granular Materials* (Cambridge University Press, Cambridge, 1992).

[2] J. Rajchenbach, in *Physics of Dry Granular Media*, H.J. Hermann, J.P. Hovi, and S. Luding, eds. (Kluwer Academic Publishers, Dordrecht,1998), p. 421.

[3] P.-G. de Gennes, in *From Rice to Snow*, Lecture at the Nishina Memorial Foundation, Publication Nr 38 (Nishina Memorial Foundation, April 1998). See also Ref. [8].

[4] F. Radjai, D. Wolf, and S. Roux, *Phys. Rev. Lett*., **77**, 274 (1996); C.H. Liu, S. Nagel, D. Shechter, S. Coppersmith, S. Majumdar, O. Narayan, and T. Witten, *Science*, **269**, 513 (1995); F. Radjai, D.E. Wolf, S. Roux, M. Jean, and J.-J. Moreau, in *Powders and Grains 97*, R. Behringer and J. Jenkins, eds., Balkema Publishers, Rotterdam, 1997), p. 211.

[5] J.-P. Bouchaud, M.E. Cates, J. Ravi Prakash, and S.F. Edwards, *J. Phys. France I*, **4**, 1383 (1994); J.-P. Bouchaud, M.E. Cates, J. Ravi Prakash, and S.F. Edwards, *Phys. Rev. Lett.*, **74**, 1982 (1995). See also A. Mehta, in *Granular Matter*, A. Mehta, ed. (Springer Verlag, Heidelberg, 1994).

[6] P.-G. de Gennes, *C. R. Acad. Sci. Paris, Ser. IIb*, **321**, 501 (1995).

[7] P.-G. de Gennes, *Cours du Collège de France*, unpublished (Collège de France, Paris, 1997).

[8] T. Boutreux, E. Raphaël and P.-G. de Gennes, *Phys. Rev. E*, **58**, 4692 (1998).

[9] T. Boutreux and E. Raphaël, *Phys. Rev. E*, **58**, 7645 (1998).

[10] J.-P. Bouchaud and M.E. Cates, in *Physics of Dry Granular Media*, H.J. Hermann, J.P. Hovi, and S. Luding eds., (Kluwer Academic Publishers, Dordrecht,1998), p. 465.

[11] L. Samson, I. Ippolito, S. Dippel, G.G. Batrouni, in *Powders and Grains 97*, R. Behringer and J. Jenkins, eds. (Balkema Publishers, Rotterdam, 1997), p. 503.

[12] S. Dippel, G.G. Batrouni, D.E. Wolf, in *Powders and Grains 97*, R. Behringer and J. Jenkins, eds. (Balkema Publishers, Rotterdam, 1997), p. 559.

[13] S. Douady, B. Andreotti, and A. Daerr, *Eur. Phys. J. B*, **11**, 131 (1999).

[14] J. Rajchenbach, E. Clément and J. Duran, in *Fractal Aspects of Materials*, F. Family, P. Meakin, B. Sapoval and R. Wool, eds., M.R.S. Symposia Proceedings No. 367 (Materials Research Society, Pittsburgh, 1995), p. 525.

[15] E. Azanza, P. Chevoir and P. Moucheron, in *Powders and Grains 97*, R. Behringer and J. Jenkins, eds. (Balkema Publishers, Rotterdam, 1997), p. 455.

[16] O. Pouliquen, *Phys. Fluid*, **11**, 542 (1999).

[17] A. Aradian, E. Raphaël, P.-G. de Gennes, *Phys. Rev. E*, **60**, 2009 (1999).

[18] T. Boutreux and P.-G. de Gennes, *J. Phys. France I*, **6**, 1295 (1996).

[19] H.A. Makse, *Phys. Rev. E*, **56**, 7008 (1998); H.A. Makse, P. Cizeau and H.E. Stanley, *Phys. Rev. Lett.*, **78**, 3298 (1997).

[20] S.B. Savage and K. Hutter, *J. Fluid Mech.*, **199**, 177 (1989).

[21] S.N. Dorogovtsev and J.F.F. Mendes, *Phys. Rev. Lett.*, **83**, 2946 (1999).

[22] L. Mahadevan and Y. Pomeau, *Europhys. Lett.*, **46**, 595 (1999).

[23] T. Emig, P. Claudin and J.-P. Bouchaud, *Europhys. Lett.*, **50**, 594 (2000).